Proceedings of Ninth World Conference on Earthquake Engineering
August 2-9, 1988, Tokyo-Kyoto, JAPAN (Vol.III)

4-3-18

A METHOD OF ONE-DIMENSIONAL ANALYSIS FOR LIQUEFACTION CONSIDERING CYCLIC MOBILITY

Masaya MIHARA and Kunio NISHI

Technical Research Institute, HAZAMA-GUMI, LTD,
Yono-shi, Saitama, Japan

SUMMARY

Often discussed in recent years is the requirement to establish the analytical method which is capable of evaluating the seismic behavior of dense sand ground accurately. Accordingly, the authors developed a numerical model incorporating the cyclic mobility by comparing the numerical results with the experimental observations of shaking table test. As a result, the model proposed by the authors showed good agreement especially in the acceleration and the pore water pressure qualitatively as well as quantitatively.

INTRODUCTION

In Japan, often discussed in recent years is the feasibility of building important structures requiring high earthquake resistance on dense sand ground such as diluvial sand, instead of only on bedrocks as in the past. Accordingly, the necessity of establishing analytical methods capable of strictly and accurately evaluating the behavior of dense sand ground during earthquakes has suddenly arised.

The authors paid attention to the behavior of dense sand ground during earthquakes, and proposed a model which could be handled as an extention from the conventional method of analyzing effective stress for loose sand. Its applicability was confirmed by making a comparison with the results of experiments.

A MODEL FOR STRESS-STRAIN RELATION DURING UNDRAINED, CYCLIC SHEAR LOADING

Making model As it is different from loose sand, the cyclic mobility significantly appears when cyclic shear loading is applied to dense sand under the undrained condition. The shear stress-shear strain curve of sand is closed to hard-spring type when the cyclic mobility appears. According to Pradhan et al. (Ref.1), it was reported that the shear stress ratio-shear strain relations expressed by taking account of the change in effective stress are always of hyperbolic type. The authors then formulated a model to express the shear stress-shear strain relations of undrained sand during cyclic loading by extending the Hardin-Drnevich model especialy to enable the model to express the relations for dense sand. The model was made on the basis of the assumptions explained below.

(1) Shear stress-shear strain relatios will be considered separately from excess pore water pressure model.

(2) As model for the generation of excess pore pressure, a model based on effec tive stress path proposed by Ishihara et al. (Ref. 2) will be used.
(3) Shear stress-shear strain relations will be defined by the extended form of Hardin-Drnevich model. For the cyclic loading, Masing's rule will be applied for the shear stress ratio-shear strain relations.

In this case,the model proposed by Ishihara et al. was adopted as an excess pore water pressure model because it was considered to be a model incorporating the cyclic mobility.

The shear stress-shear strain model consists of a skeleton curve for monotonous loading and a hysteresis curve for cyclic loading. The skeleton curve of the Hardin-Drnevich model is normally expressed by Eq. (1).

$$\tau=\frac{1}{\frac{1}{G_{max}\cdot\gamma}+\frac{1}{\tau_{max}}} \tag{1}$$

where, Gmax: Initial shear stiffness. τ_{max} : Shear strength.

In this case, it is assumed that Gmax and τ_{max} , as functions of effective stress, can be expressed by Eq.(2) and (3).

$$G_{max}=G_0'\cdot\sigma_v'^{n} \tag{2}$$

$$\tau_{max}=\sigma_v'\tan\phi \tag{3}$$

where, n : Constant (0< n <1).
G_0': Constant (function of void ratio, K value,etc.).
ϕ : Internal friction angle

The authors divided the expressions at both the sides of Eq.(1) by σ_v' . Eq.(4) , which is expressed using the relation of Eq.(2) and (3), is considerd to be the skeleton curve which takes account of change in the effective stress.

$$\frac{\tau}{\sigma_v'}=\frac{1}{\frac{1}{\frac{G_0'}{\sigma_v'^{1-n}}\cdot\gamma}+\frac{1}{\tan\phi}} \tag{4}$$

With respect of the hysteresis curve, Masing's rule is applied to Eq.(4) and then Eq.(5) is defined because the shear stress ratio-shear strain relation is of hyperbolic type.

$$\frac{\frac{\tau}{\sigma_v'}-\frac{\tau^*}{\sigma_v'^*}}{2}=\frac{1}{\frac{1}{\frac{G_0'}{\sigma_v'^{1-n}}\cdot\frac{\gamma-\gamma^*}{2}}\pm\frac{1}{\tan\phi}} \tag{5}$$

where, double sign is :
Positive when strain increases (rising curve)
Negative when strain decreases (falling curve)
τ^* , γ^* and $\sigma_v'^*$ are the values of τ , γ and σ_v' at preceding returning points.

Soil constant n Examples of calculation with 2 kinds of n (n=0.4 & 0.75) for cyclic loading under undrained condition by using the proposed model will be explained below. Table 1 shows the list of common parameters used in calculations, and Fig.1 shows the model for generation of excess pore water pressure. Also, Fig.2 indicates the shear stress-shear strain relationship when n=0.4 and 0.75. As shown in Fig.2, the shear stress-shear strain relations indicate the shape of the hard-spring type can be expressed more strongly as n become larger. Fig.3 indicates the shear stress ratio-shear strain relationship. It can be known that both cases exhibit the spindle shape.

Table. 1 Physical values

σ_v' (tf/m²)	τ_a (tf/m²)	G_o' (tf/m²)$^{1-n}$	B_p	B_u	θ_s	ϕ_l	ϕ
10.0	2.0	2000.	1	0.5	27°	32°	34°

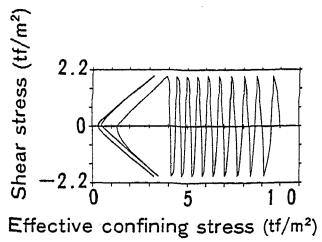

Fig. 1 Pore pressure generation model

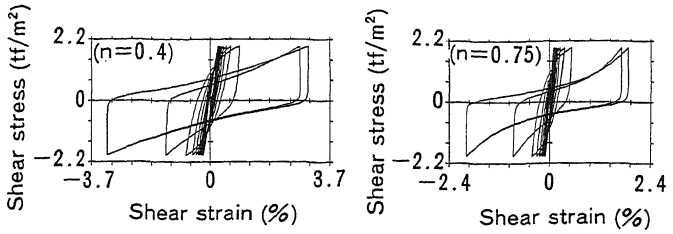

Fig. 2 Stress-strain relation

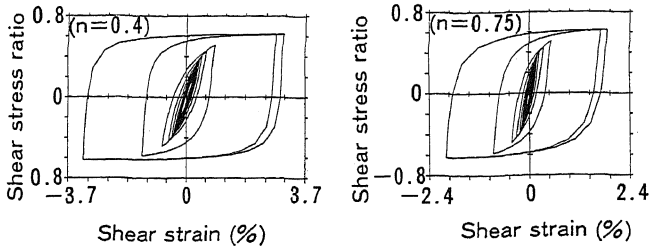

Fig. 3 Stress ratio-strain relation

The proposed model satisfies the shear stress-shear strain relationship of the hyperbolic type by the Hardin-Drnevich model as the behavior under drained condition, where the effective stress does not vary, and can also express the shear stress-shear strain curve of the hard-spring type as the behavior under undrained condition when the effective stress varies. Therefore, the model can handle both the undrained and drained conditions in an unified manner and may therefore be handled more easily when it is to be incorpolated into a response analysis program.

One-Dimensional Analysis Program A one-dimensional analysis program incorporating the proposed model was formulated. For the formulation, the ground was assumed as a one-dimensional continuous body, and the nonlinear equations was solved with step-by-step integration. Its discretization formula is shown in Eq.(6).

$$\boldsymbol{M}\ddot{\tilde{\boldsymbol{u}}}_j+\boldsymbol{C}\dot{\tilde{\boldsymbol{u}}}_j+\boldsymbol{T}_{j-1}+\boldsymbol{K}_j\Delta\tilde{\boldsymbol{u}}_j=-\boldsymbol{M}\boldsymbol{J}\ddot{u}_{N,j} \tag{6}$$

where, $\Delta\tilde{\boldsymbol{u}}_j=\tilde{\boldsymbol{u}}_j-\tilde{\boldsymbol{u}}_{j-1}$, $\boldsymbol{T}_j=\sum_{i=1}^{j}\boldsymbol{K}_i\Delta\tilde{\boldsymbol{u}}_i$

$\tilde{\boldsymbol{u}}$: Relative displacement vector
$\boldsymbol{C}$: Damping matrix
$\ddot{u}_N$: Acceleration of foundation bed
$\boldsymbol{M}$: Mass matrix
$\boldsymbol{J}$: J matrix
$\boldsymbol{K}_j$: Stiffness matrix of j-th step

The tangent shear stiffness Gt of each layer forming stiffness matrix is given by Eq.(7), considering the change of effective confining pressure σ_v'.

$$G_t=\frac{d\tau}{d\gamma}=\frac{G_0'\cdot\sigma_v'^{n}}{R}\left(1-\frac{T-T^*}{\Theta\cdot\tan\phi}\right)^2 \tag{7}$$

$$R=1-\left\{nT+(1-n)T^*+\frac{(1-n)(T-T^*)^2}{\Theta\cdot\tan\phi}\right\}\frac{d\sigma_v'}{d\tau}$$

where, $T=\frac{\tau}{\sigma_v'}$, $T^*=\frac{\tau^*}{\sigma_v'^*}$

Θ = 1 for rising curve in skeleton curve
= 2 for rising curve in hysteresis curve
= -1 for falling curve in skeleton curve
= -2 for falling curve in hysteresis curve

Outline of Experiments and Physical Values Used in Analysis Outline of the model used in experiments and the location of the instruments installed are shown in Fig.4.Toyoura sand was used for the saturated sand ground. The specimen (30 cm wide, 60 cm long, 60 cm high) was made in a special soil container for shear vibration with water-pluviation method, and the container was placed on a shaking table. Vibration with a SIN wave of 3 Hz frequency and an acceleration of about 150 gal was given. Measurments were made for the acceleration and pore water pressure in the specimen.

The physical values employed for the simulation were determined as explained below. At first, Ishihara's model was used as the model for the pore water pressure generation in the model proposed by the authors. Therefore, the parameters related to the model for pore water pressure generation were determined after making a parameter study for the results of the cyclic shearing test under the undrained condition for Toyoura sand having a relative density almost as same as that in the experiment. The time history of pore water pressure during test is compared to the time history of pore water pressure by simulation in Fig.5. Also, if Ishihara's model is used as it is for the rising process of pore water pressure after reaching the phase transformation line, the quantity of rising become larger than the test results. Because of this, the rate rising of the pore water pressure during unloading was made one-fourth of the Ishihara's model.

For other physical values, the values estimated from the relative density was used. A list of physical values used in the analysis as well as the condition of analysis are indicated in Table 2.

Results of Simulations Fig. 6b) shows the response acceleration waveforms at the ground surface and at a depth of 30 cm. By comparing them to the experiment results in Fig. 6a), it will be known that the magnitude of response acceleration and the pattern of change in time history exhibit almost the same tendencies. Especially in the surface layers, the unusual rising of acceleration and the decrease in response acceleration can be recognized. The response values at the depth of 30 cm almost agree up to about 4 seconds but thereafter, the calculated results tend to show the unusual rising more quickly and the occurrence of maximum response in an earlier stage.

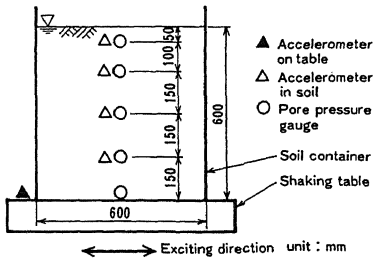

Fig. 4 Specimen and measurements

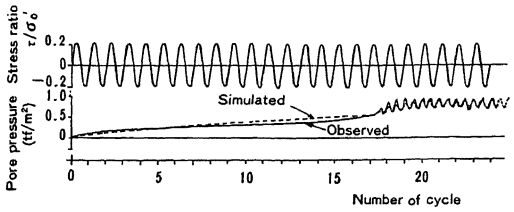

Fig. 5 Cyclic shearing test and its simulation

Table. 2 Condition of simulation

depth (cm)	layer	nodal plane	γ_t (tf/m³)	G_o' (tf/m²)$^{1-n}$	parameters
±0	①	0	1.8	1180	$B_p = 1.35$ $B_u = 0.56$ $n = 0.9$ $\theta_s = 16.5°$ $\phi = 38.0°$ $\phi_t = 36.0°$ $\Delta t = 0.0001$ (sec) base acceleration sin wave (3 Hz) 150 gal
	②	1			
	③	2			
	④	3			
	⑤	4			
−60	⑥	5			

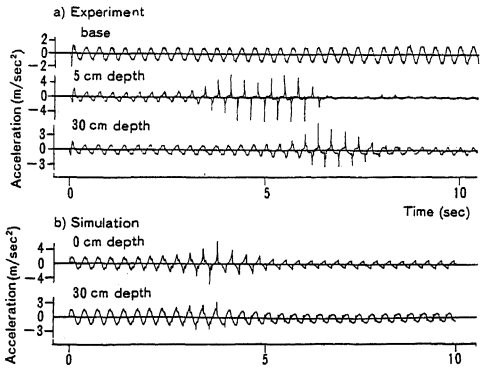

Fig. 6 Time histry of acceleration.

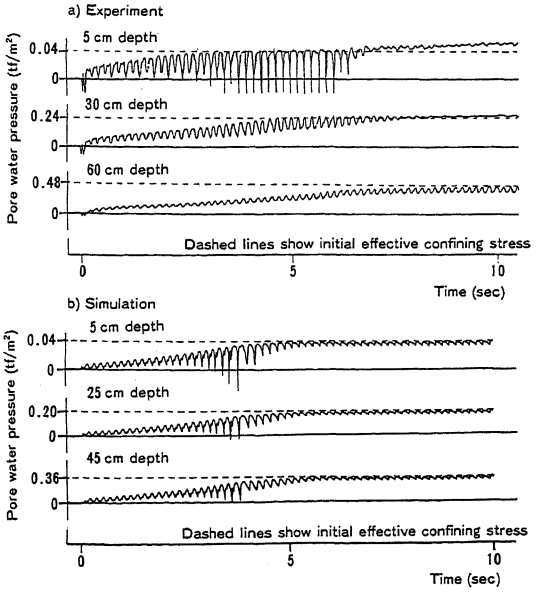

Fig. 7 Time histry of pore water pressure

Fig. 7b) shows the excess pore water pressure waveforms at the depth 5 cm, 25 cm and 45 cm. When comparing them to the results of experiments in Fig. 7a), the rising process of pore water pressure agrees fairly well between them. However, according to a detailed comparison, the excess pore water pressure rises almost in the same manner regardless of the depth in simulation. On the other hand, in the experiments, the time to reach the upper limit of excess pore water pressure is longer in the lower layers. This difference is probably caused because the dissipation of the excess pore water pressure is not taken into account in the simulation.

Fig. 8 and Fig. 9 show the calculated time history waveform of the shear strain as well as shear stress-shear strain curves. From Fig. 8 it can be known that strain gradually increase as the pore water pressure rises and that strain suddenly increases immediately before the pore water pressure reaches the maximum value. Fig. 9 shows the curve of the hard-spring type in the middle. It is recognized from Fig. 6 and Fig. 9 that the acceleration waveform has unusual rises when the shear stress-shear strain curve shows a hard-spring type and thereafter, the acceleration decreases as the shear stiffness become smaller.

In the foregoing paragraphs, the results of simulation are indicated, and both the response acceleration and excess pore water pressure are compared to the results of experiments. As a consequence, the results of simulation using the proposed model indicate that the response acceleration shows an unusual shape and decrease thereafter and that the rising process of excess pore water pressure and the relative behavior between response acceleration and excess pore water pressure qualitatively agree fairly well the results of experiment. It can be said that the time history of the shear strain and the shear stress-shear strain curves well express the experimental values except for the rate of rising of excess pore water pressure in the lower layers, and for the peak value when the response acceleration indicates an unusual shape.

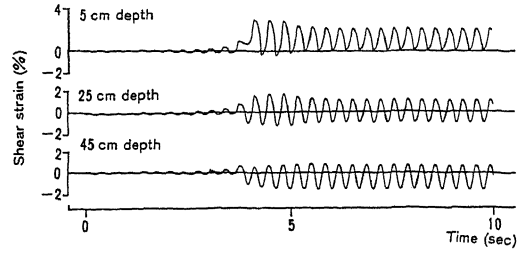

Fig. 8 Time histry of shear strain

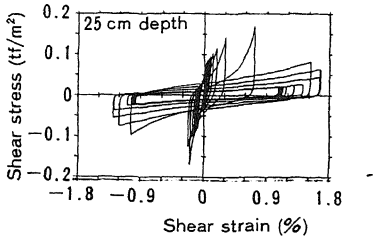

Fig. 9 Stress-strain relation

POSTSCRIPT

This study was made in order to apply the conventional method of effective stress analysis for loose sand to dense sand also. As a result, the model proposed by authors may be highly evaluated from the qualitative viewpoint, which has become apparant through comparison to the results of expriments. Also, in the quantitative aspect, the results agree fairly well with the results of experiments within the range of comparison actually made.

The authors will further confirm the quantitative applicability of this approach by comparing with results of experiments and results of future earthquake obsevation.

REFERENCES

1. Pradhan, T.B.S., Tatsuoka, F., and Hara, K., "Stress-Strain Characteristics of Sand in Cyclic Torsional Shearing under Undrained Condition, "Proc. of the 42 st Annual Conf. of JSCE, 3, 25-26, (1985)
2. Ishihara, K., and Touhata, I., "One-Dimensinal Soil Response Analysis during Earthquake Based on Effective Stress Method, "Journal of the Faculty of Engineering, University of Tokyo (B), Vol.35, No. 4, (1980)
3. Mihara, M. and Nishi, K., "One-Dimensional Liquefaction Analysis Considering a Cyclic Mobility, "Technical Research Report of HAZAMA-GUMI, LTD., -1986, 113-124, (1986)